THE UNIVERSITY *of* EDINBURGH

Edinburgh Research Explorer

A direct neurokinin B projection from the arcuate nucleus regulates magnocellular vasopressin cells of the supraoptic nucleus

A direct neurokinin B projection from the arcuate nucleus regulates magnocellular vasopressin cells of the supraoptic nucleus

Rafael Pineda Reyes[1], Nancy Sabatier[1], Mike Ludwig[1], Robert P. Millar[2], and Gareth Leng[1]

[1]Centre for Integrative Physiology, University of Edinburgh, Hugh Robson Building, George Square, Edinburgh EH8 9XD, UK

[2]Mammal Research Institute, Department of Zoology and Entomology, University of Pretoria, Pretoria 0001; MRC Receptor Biology Unit, Institute for Infectious Diseases and Molecular Medicine, University of Cape Town, Cape Town 7925, South Africa

Corresponding author and person to whom reprint requests should be addressed:

Mike Ludwig

Centre for Integrative Physiology

University of Edinburgh

Hugh Robson Building, Edinburgh EH9 2XD, UK

Phone: 0044 131 650 3275

Email: mike.ludwig@ed.ac.uk

Abstract

Central administration of neurokinin B (NKB) agonists stimulates immediate early gene expression in the hypothalamus and increases secretion of vasopressin from the posterior pituitary through a mechanism that depends on the activation of neurokinin receptor 3 receptors (NK3R). Here we report that, in the rat, immunoreactivity for NK3R is expressed in magnocellular vasopressin and oxytocin neurones in the supraoptic nucleus (SON) and paraventricular nucleus (PVN) of the hypothalamus, and that NKB immunoreactivity is expressed in fibres in close juxtaposition with vasopressin neurones at both of these sites. Retrograde tracing in the rat showed that some NKB-expressing neurones in the arcuate nucleus project to the SON, and in mice, using an anterograde tracing approach, we found that kisspeptin-expressing neurones of the arcuate nucleus, which are known to co-express NKB, project to the SON and PVN. Finally, we show that i.c.v. injection of the NK3R agonist senktide potently increases the electrical activity of vasopressin neurones in the SON *in vivo* with no significant effect detected on oxytocin neurons. The results suggest that NKB-containing neurones in the arcuate nucleus regulate the secretion of vasopressin from magnocellular neurons in rodents, and we discuss the possible significance of this.

Introduction

The peptide hormone vasopressin is synthesised in magnocellular neurosecretory neurones in the supraoptic (SON) and paraventricular (PVN) nuclei of the hypothalamus, and is the main hormonal regulator of plasma osmolality and body water content. In the elderly, about half of all cases of chronic hyponatremia are attributed to chronically elevated secretion of vasopressin (1). In humans, vasopressin secretion progressively increases with age (2, 3), and the size of magnocellular vasopressin neurons in the SON and PVN is increased after the age of 60 years, suggesting that there is also an increase in vasopressin production (2, 4). In aged rodents, there is also an increase in vasopressin secretion, and this has been linked to impaired osmoregulation (5). Aging is also associated with a marked decline in sex steroid production in both men and women, but whether the age-related increase in vasopressin synthesis and secretion is linked to age-related decline in sex steroid production is not known.

In this study, we explored neuroanatomical and functional interactions between neurons that express neurokinin B (NKB) and magnocellular vasopressin neurons. NKB, a member of the tachykinin neuropeptide family, is a critical regulator for the central control of reproduction. The

biological effects of tachykinins are mediated by three different neurokinin receptors: NK1R, NK2R, NK3R, and NKB preferentially binds to NK3R (6). The earliest evidence of a role for NKB in human reproduction came from a study of postmenopausal women by Rance and Young (7) which demonstrated hypertrophy and hyperplasia of cells containing NKB in the infundibular nucleus – the nucleus homologous to the arcuate nucleus in rodents. Similar results have since been found in the infundibular nucleus of the aging man (8). This led to the recognition that NKB expression is inversely correlated to levels of circulating sex steroids. Thus, for example, NKB expression is greatly elevated by gonadectomy in a manner reversible by replacement with sex steroids (9). A similar pattern has been described in monkeys, where ovariectomy results in neuronal hypertrophy and an increase of *NKB* mRNA expression (10). In addition, gonadal steroids have been reported to have marked effects on the somata and dendrites of arcuate nucleus NKB neurons (11).

There is already considerable evidence that the NKB/NK3R system may regulate vasopressin secretion. Central injection of a selective NK3R agonist, senktide, induces antidiuresis by increasing peripheral vasopressin secretion (12), whereas neurokinin A, substance P and selective NK-1 agonists have no such effect. The actions of senktide are likely to be direct, as mRNA for NK3R is expressed in both the SON and PVN (13), and as senktide can also stimulate vasopressin secretion from explants of the hypothalamo-hypophysial system (14). Conversely, central administration of a NK3R antagonist reduces osmotically-stimulated vasopressin secretion in rats (15).

In this study, using immunocytological and electrophysiological approaches, we aimed to determine 1) whether there is an anatomical connection between the NKB-producing neurones in the arcuate nucleus and vasopressin neurones in the SON and PVN, and 2) the effects of the NK3R agonist, senktide, on the electrical activity of magnocellular vasopressin and oxytocin neurones in the SON.

Materials and Methods

Experiments were performed on adult male Sprague–Dawley rats (body weight ~ 300 g) and adult male transgenic *Kiss1/*Cre-eGFP mice (body weight ~ 30 g) that had been housed on a 12:12 h light:dark cycle (lights off at 19.00 h) with free access to food and water. All experiments were conducted in accordance with a UK Home Office project licence that has been reviewed by the University of Edinburgh Ethics Committee.

Tracing/Connectivity studies

For retrograde tracing experiments, we used retro-beads as they show very limited spread from the injection site, and do not need an antibody for detection (16). The injection method we used is described in detail elsewhere (17). Rats were anesthetized first with 4% isoflurane and then

maintained on 1.5 – 2% isoflurane. They were placed in a stereotaxic frame and a glass capillary was implanted in SON using the following coordinates (18): anterioposterior -1.3 mm; mediolateral 2.0 mm; dorsoventral 9.4 mm. Red retro-beads (Lumafluor, Inc.) were injected in the SON (100 nl) by pressure injection. Once the wound was sutured, rats were given buprenorphine (0.03 mg/kg) subcutaneously. One week after injection, the rats were transcardially perfused, and the brains were removed and processed for immunofluorescence as described below.

Anterograde tracing

Recombinant adeno-associated virus vectors (rAAVs) have been commonly used to deliver genes of interest into the central nervous system *in vivo*. Here we used a cre-dependent approach to deliver YFP specifically to arcuate nucleus kisspeptin neurons (19, 20). Kisspeptin-expressing neurons in the arcuate nucleus of rodents (21, 22), sheep (23), and monkey (24) co-express NKB and dynorphin. Using this property of arcuate kisspeptin neurons, we used the transgenic *Kiss1/*Cre-eGFP knock-in mouse (25) to trace kisspeptin arcuate nucleus projections to the SON and PVN.

We used an AAV where an inverted YFP reporter sequence was floxed by two LoxP sequences oppositely oriented. Thus, after the cre-recombinant event in kisspeptin cells, YFP was orientated to the correct sense and transduced specifically in cre cells only under the constitutively-expressed elongation factor 1-alpha promoter (Ef1a) (26, 27). This type of AAV, commonly known as a DIO-AAV, was purchased from Gene Therapy Center Vector Core (University of North Carolina; serotype 5; viral titer 10^{12} vg/ml). Using a similar approach to that described in the retrograde tracing study above, *Kiss1/*Cre-eGFP mice were injected with 300 nl of the DIO-AAV into the arcuate nucleus following the coordinates (28): anterioposterior -1.8 mm; mediolateral 0.3 mm; dorsoventral 5.8 mm. Although this transgenic line expresses eGFP under the kisspeptin promoter, this expression is restricted to the nucleus, thus, any YFP projections found come from the AAV-DIO-YFP. Three weeks after injection, mice were perfused transcardially with paraformaldehyde, and the brains were removed and processed for double immunofluorescence as described below.

Immunofluorescence protocols

Adult male rats (body weight ~300 g) and adult male *Kiss1/*Cre-eGFP mice were injected with a lethal dose of sodium pentobarbitone and transcardially perfused with heparinised 0.9% saline, followed by 4% paraformaldehyde in 0.1 M phosphate-buffered saline (pH 7.3-7.4). Brains were extracted and post-fixed overnight at 4ºC in 2% PFA + 15% sucrose solution then cryoprotected in 30% sucrose in PBS with 0.01% sodium azide. Coronal brain sections (40 μm) were cut on a freezing microtome.

For NK3R and NKB immunoreactivity studies, sections were mounted on SuperFrost Plus slides then dried for 1 h at 37ºC. Sections were washed in PBS-T (0.1% Tween-20) for 10 min at room temperature. Heat-induced epitope retrieval (HIER) was then performed in 10 mM sodium citrate pH 6 for 10 min at 90ºC. Afterwards, sections were cooled to room temperature and then washed for 5 min in PBS at room temperature. The sections were incubated in blocking buffer (3% donkey or goat serum, 0.4% Triton X-100 in PBS) for 45 min at room temperature. Next, the sections were incubated with primary antibodies (Table 1) in blocking buffer for two days at 4ºC, then washed three times for 10 min in PBS. Finally, the sections were incubated with secondary antibodies (Table 1) in blocking buffer for 1 h at 37ºC, then washed three times for 10 min in PBS, and mounted on slides using PermaFluor Aqueous Mounting Medium (Thermo Scientific, TA-030-FM). No signal was detected after applying secondary antibodies in the absence of primary antibodies.

For the anterograde tracing study using AAV, we used the same protocol as described above but without the HIER step. The anterograde tracing study did not allow us to use simultaneously visualize NKB by immunohistochemistry. While the specificity of the NKB antibody is high, its sensitivity is low, and we were able to label fibres only after the HIER step, which compromises the detection of YFP.

For the retrograde tracing study, we used free-floating sections. Sections were washed twice for 10 min in 0.1 M PB, then incubated for 30 min in freshly made 1% (w/v) sodium borohydride in 0.1 M PB, and washed four times for 10 min in 0.1 M PB They were then incubated 30 min in 0.1 M Glycine and washed four times for 10 min in 0.1 M PB followed by 45 min in blocking solution of 3% donkey serum + 0.4% triton X-100 in 0.1 M PB. Next, free-floating sections were incubated with primary rabbit NKB antibody (Table 1) diluted in blocking buffer for 2 days at 4ºC. After incubation with the primary antibody, sections were washed four times for 10 min in 0.1 M PB, followed by a 2 h incubation with secondary anti-rabbit antibody Alexa 488 (Table 1). Finally, sections were mounted in SuperFrost Plus slides using Fluoromount (Sigma -F4680) after washing. All incubations were at room temperature unless stated.

Immunoreactivity was visualized on the Nikon A1R FLIM confocal system. Images were viewed and Z stacks condensed to maximum intensity projections using NIS-Elements Viewer software. Resulting images were exported to the ImageJ software. To facilitate color-blind readers, the red channel was recolored to magenta; overlay of green and magenta channels results in a white colour channel.

Table 1: Primary and secondary antibodies used in the immunofluorescence assays.

Primary Abs	Code	Supplier	Dilution	Raised in:
Vasopressin-neurophysin	PS41	Dr H Gainer	1/500	mouse
Oxytocin-neurophysin	PS38	Dr H Gainer	1/500	mouse
NK3R	IS-7/7	Dr Philippe Ciofi	1/3,000	rabbit
NKB	NB300-201	Novus Biologicals	1/800	rabbit
GFP/YFP	Ab13970	Abcam	1/10,000	chicken
Secondary Abs	Code	Supplier	Dilution	Raised in:
Alexa Fluor® 488 Anti-Rabbit	A-21206	Life Technologies	1/500	donkey
Alexa Fluor® 555 Anti-Mouse	A-31570	Life Technologies	1/500	donkey
Alexa Fluor® 488 Anti-Chicken	A-11039	Life Technologies	1/500	goat
Alexa Fluor® 555 Anti-Mouse	A-21422	Life Technologies	1/500	goat

In vivo electrophysiology

Adult male rats were anesthetized with urethane (1.25 g/kg, i.p.), a femoral vein was cannulated and a catheter was inserted in the trachea. The SON and an area rostral to the pituitary and on the midline were exposed transpharyngeally, as described fully elsewhere (29). A microinjection cannula was placed 0.5-1 mm rostral to the neural stalk and on the midline then lowered into the third ventricle to inject 600 pmol of senktide in a volume of 2 µl over 100 s. Under visual control, a glass microelectrode (tip diameter ~ 1 µm) filled with 0.9% NaCl was placed in the SON to record from single neurones using conventional extracellular recording techniques.

In this study, unlike our previous electrophysiological studies on SON neurones, we could not identify these neurones antidromically as projecting to the posterior pituitary gland because inserting a microinjection cannula ventrally into the 3rd ventricle did not leave enough space to also place a stimulating electrode on the neural stalk and a recording electrode in the SON. We therefore used other ways to ensure that we recorded from magnocellular neurones: 1) the ventral approach allows us to visually place the recording electrode on the surface of the brain just below the SON (which, unlike the PVN, contains only magnocellular neurons); 2) phasically firing cells in this area can only be magnocellular vasopressin neurones; 3) we checked the shape of interspike-interval histograms and hazard functions of the recorded cells, as these reveal the characteristic firing patterns of SON vasopressin and oxytocin neurones as shown previously (30). Oxytocin cells were distinguished from vasopressin cells by their firing pattern and by their opposite response to intravenous CCK [20 μg/kg; cholecystokinin-(26-33)-sulfated; Bachem, Essex, UK]. In phasic neurones, burst patterning (activity quotient and intraburst firing rate) was analysed as described elsewhere (30).

Responses to senktide were analysed by comparing the mean firing rate in 10-min intervals after senktide injection with the (basal) firing rate measured in a 10-20 min control period before senktide injection. Only one injection of senktide was made in each experiment, so the results shown are those from individual rats. Responses to senktide were very prolonged, and we quantified effects by comparing activity in the period between 20 and 40 min after injection with the activity in the 10 min before injection, and tested the significance of differences using a 2-tailed Mann-Whitney test. For phasic firing neurones, bursts were recognized by a conventional algorithm (30) according to the criteria: minimum length 3 s; minimum interburst period 3 s; maximum intraburst interspike interval 1 s; minimum 20 spikes per burst; maximum interval at start of burst 0.8 s. Having identified bursts and silences, we calculated the activity quotient (AQ = time active / time recorded) and the intraburst spike frequency. For all neurones, we constructed interspike interval histograms (in 5-ms bins) for the periods analysed, and then constructed hazard functions according to the formula (hazard in bin [t, $t+$ 5]) = (number of intervals in bin [t, $t+$ 5])/(number of intervals of length > t).

Results

NK3R and NKB immunoreactivity in the SON and PVN.

In the SON and PVN (Fig 1,2), we found dense expression of NK3R immunoreactivity whereas the surrounding perinuclear zones were apparently devoid of NK3R immunoreactivity, indicating a strong and specific expression of NK3R in magnocellular neurones. Within the SON and PVN, the immunoreactivity was mainly absent from cell nuclei, and apparently mainly (but not exclusively) localised to the neuronal cell membranes (Fig 1D, 2D). In both nuclei, NK3R expression

was co-localized with both vasopressin-neurophysin (Fig. 1) and oxytocin-neurophysin (Fig. 2). NK3R expression was also found in all the accessory magnocellular nuclei including in the nucleus circularis, and in the retrochiasmatic part of the SON (images not shown). In the SON, NK3R was expressed in all neurones, but in the PVN it was preferentially expressed in vasopressin cells (Fig 1C, Fig. 2C). To quantify this, we analysed sections of the PVN from three rats, sampling cells that expressed vasopressin-neurophysin or oxytocin-neurophysin, and which could be unambiguously defined as NK3R-positive or NK3R-negative. Of 111 vasopressin cells, 99 co-expressed NK3R (89%), whereas of 128 oxytocin cells, only 36 (28%) co-expressed NK3R.

Consistent with previous studies, we observed a large population of NKB-expressing cells in the caudal arcuate nucleus (not shown). NKB-positive fibers from these cells passed through the rostral arcuate nucleus, and some of these could be seen to enter the caudal region of the SON (Fig. 3A); other fibres coursed dorsally towards the PVN alongside the walls of the third ventricle (Fig 3A). Within both the SON and PVN, we found abundant expression of NKB-expressing fibres with boutons in close juxtaposition to vasopressin cells (Fig. 3B,C). However, we did not find any NKB-expressing cell bodies in either of these nuclei.

Projections of NKB-expressing cells from the arcuate nucleus

Retrograde study These immunohistochemical studies suggested that at least some of the NKB projections found within the SON originated from NKB-expressing cells in the caudal arcuate nucleus. To test this, we aimed to inject retro-beads into one SON side in six rats, and present here the results from two rats in which the injection was on target with minimal spread outside the SON (Fig. 4A). We used a small volume of retro-beads to achieve higher specificity, so we expected to inject only a small area of the SON and therefore only a few fibres were likely to uptake the beads. A week after injection, retro-beads injected into the SON were found in the cytoplasm of 11% of NKB-expressing cells (27 out of 238 cells) in the caudal arcuate nucleus (Fig. 4B-F).

Anterograde study We injected a cre-dependent AAV-DIO-YFP in the arcuate nucleus of three *kiss1*-Cre/eGFP mice, and present here the results from two mice in which the injection was on target (Fig. 5A). We found YFP-expressing fibers in the PVN and SON (Fig. 5B,C), indicating that some kisspeptin-expressing cells in the arcuate nucleus project to both these nuclei in mice.

Effect of NKB on the electrical activity of SON vasopressin and oxytocin neurones

In the SON of urethane-anaesthetised rats we recorded from 17 vasopressin neurones (mean basal rate 5.1 ± 0.76 spikes/s), of which 10 were firing phasically and seven were firing continuously. Those firing continuously were identified as vasopressin neurones by their response to CCK (inhibition or no response) and by analysing the nature of their firing pattern: hazard functions constructed from interspike interval data revealed the presence of a post-spike hyperexcitability that is uniformly present in vasopressin neurones (30) but mainly absent from oxytocin neurones (Fig. 6B).

Of the 17 neurones, one phasic neurone was lost at 10 min after senktide injection, after increasing its firing rate from 8.0 to 9.7 spikes/s in that time. The other 16 neurones were all kept for between 30 and 60 min after injection, and the mean firing rate of these, averaged over 20-40 min after injection, was 2.1 ± 0.7 spikes/s higher than the basal rate (Fig. 6A and C; $P = 0.008$, Mann-Whitney test).

The nine phasically firing neurones that were held for more than 30 min had a mean basal rate 3.3 ± 0.7 spikes/s (range 0.5 - 8 spikes/s); this activity comprised bursts and intervening silences, and to assess whether the response to senktide was due to a change in the burst length or/and a change in burst intensity we analysed the changes in the activity quotient (AQ = time active / time recorded) and in the intraburst frequency. The AQ was raised by 0.19 ± 0.11 from 0.49 ± 0.07 to 0.68 ± 0.1 at 20-40 min after senktide injection (Fig. 6E), and intraburst frequency was increased by 1.1 ± 0.6 spikes/s from 6.2 ± 0.5 spikes/s to 7.3 ± 0.7 spikes/s (Fig. 6F).

The seven continuously firing vasopressin neurones had a mean basal firing rate of 7.5 ± 1.7 spikes/s (range 1.9 - 10.7 spikes/s). Between 20 and 40 min after senktide injection, the mean firing rate was 1.7 ± 0.7 spikes/s higher than basal; in one of these neurones the firing rate was lower (by 0.9 spikes/s), but in five of the neurones it was increased by at least 1.5 spikes/s.

We also recorded from seven putative oxytocin neurones (mean basal rate 5.25 ± 0.8 spikes/s; range 2.6 - 6.9 spikes/s), all of which were recorded in close proximity to identified vasopressin neurones, and which were identified either by their excitatory response to i.v. CCK or by the shape of their interspike-interval histograms and resulting hazard functions (30). Overall, senktide had no significant effect on the electrical activity of these neurones (mean change at 20-40 min after senktide, -0.2 ± 0.7 spikes/s; Fig. 6C).

Discussion

Here, we confirmed that, in the rat, as previously reported (31), neurokinin receptor NK3R is densely expressed in vasopressin and oxytocin cells in the SON and PVN. We also confirmed that, in the PVN, NK3R is expressed by most vasopressin cells but by only some oxytocin cells (32); but in the SON it appeared that all neurones, including all oxytocin cells, express NK3R. NKB was expressed in fibres in close juxtaposition with vasopressin cells in both the SON and PVN. However, we failed to find NKB expression in cell bodies in either the SON or the PVN, in accord with *in situ* hybridisation studies which failed to detect *NKB* mRNA expression in these nuclei (33-35), but in contradiction to a previous study which reported co-immunostaining of NKB and vasopressin in SON and PVN neurones (36). We also showed that some NKB-expressing cells in the rat arcuate nucleus project to the SON, and in mice, we found by anterograde tracing that arcuate kisspeptin-expressing cells, which are known to co-express NKB, project to both the SON and PVN.

Finally, we showed that i.c.v. injection of the NK3R agonist senktide increases the electrical activity of vasopressin neurones but not oxytocin neurones in the SON. This is consistent with previous studies showing an increase in vasopressin secretion after i.c.v. administration of selective NK3R agonists (37), and an increase in Fos expression in the SON and PVN after i.c.v. administration of senktide (10, 38). Here we used a dose of senktide ($\sim$ 0.5 μg) that has been reported to be maximal for inducing Fos expression in the SON and PVN (38).

It has previously been reported that i.c.v injections of senktide stimulate oxytocin secretion into the plasma, but this appears to be an indirect effect as it could be blocked by the adrenergic antagonist phentolamine (39). The significance of NK3R expression in magnocellular oxytocin neurones thus remains uncertain; it appears not to be able to activate dendritic oxytocin release as, in the same study, no release of oxytocin within the PVN was found by microdialysis in response to senktide. In vasopressin cells, NK3R receptors are internalised after ligand binding and subsequently translocated to the nucleus (40). Interestingly, both hyperosmotic stimulation (40, 41) and hypotension (40) as well as senktide result in translocation of NK3R from the cytoplasm to the nucleus of vasopressin cells in the SON and/or PVN. This raises the possibility that in diverse physiological circumstances NK3R has a role in transcriptional regulation in vasopressin cells (42), and perhaps also in oxytocin cells.

Connections between the arcuate nucleus and the SON have been shown anatomically and electrophysiologically in previous studies; in particular, the SON is innervated by β-endorphin- and ACTH-containing fibres originating from the arcuate nucleus (43, 44). Electrical stimulation of the arcuate nucleus results in a complex response in SON neurones characterised by a fast inhibitory component, mediated by GABA, and a slower excitatory component (45, 46). The mediator of this

excitatory component is not known, but the present data suggest that NKB may contribute to this component of the activation in vasopressin neurones.

In neurones of the arcuate nucleus, NKB is co-localised with kisspeptin and dynorphin, so projections of this pathway to oxytocin and vasopressin neurones may have different actions depending on which receptors are present postsynaptically, and possibly also depending on differential targeting of peptides to secretory vesicles at different sites. Dynorphin is likely to be inhibitory to both oxytocin and vasopressin neurones in the SON via its actions at kappa-opioid receptors that are expressed on both of these neuronal types (47), but the effects of kisspeptin are less clear. Intravenous kisspeptin has excitatory effects on most oxytocin neurones in the SON but on only a minority of vasopressin neurones (48), but that same study reported no significant effect of i.c.v. kisspeptin on either oxytocin or vasopressin neurones in the SON, suggesting that the effects of intravenous kisspeptin were mediated indirectly, possibly via the vagus. However a subsequent study by the same authors suggested that an excitatory action of i.c.v. kisspeptin on oxytocin neurones of the SON is apparent in late pregnancy and lactation (49). The physiological significance of this is not clear: it may be, as the authors suggested, that kisspeptin has a specific role in lactation, perhaps in supporting bursting activity in response to suckling and during parturition. However, as lactation is apparently associated with a downregulation of kisspeptin and NKB expression in the arcuate nucleus (50), it may also be that the heightened responsiveness of oxytocin neurones to kisspeptin in lactation reflects upregulation of NK3R expression in response to ligand withdrawal.

Thus the physiological role of the NKB projection to the SON is, at present, unclear, but because this projection is conspicuously modulated by gonadal steroids, it seems possible that it mediates the influence of gonadal steroids on the expression and secretion of vasopressin and/or oxytocin. Neither the magnocellular oxytocin neurones nor the magnocellular vasopressin neurones express the classical oestrogen receptor, yet the synthesis of oxytocin and the secretion of both oxytocin and vasopressin are modulated by oestrogen (51-53).

Vasopressin regulates water uptake in the distal renal tubules and elevated levels can result in hyponatremia. In the elderly, hyponatremia, the most common electrolyte disorder, can be a serious health burden: common complications include an increased incidence of falls resulting from mental confusion, and osteoporosis, together giving an increased risk of fractures. About half of all cases of chronic hyponatremia are attributed to chronically elevated secretion of vasopressin (1, 2): in humans, vasopressin secretion progressively increases with age (3, 5), and the size of magnocellular vasopressin neurones in the SON and PVN is increased after the age of 60 years, suggesting that there is also an increase in vasopressin production (2). In aged rodents, there is also an increase in vasopressin secretion, and this has been linked to impaired osmoregulation (54).

Aging is also associated with a marked decline in sex steroid production in both men and women. This decline leads to an increase in the expression of NKB in the hypothalamus of humans and rodents alike, and may contribute to the progressive rise in vasopressin secretion that accompanies aging (2). In aging, chronic hyponatremia resulting from inappropriately increased vasopressin secretion has been causally linked to osteoporosis, as has reduced gonadal steroid secretion. Osteoporosis has an incidence peak in advanced age, particularly in postmenopausal women (55), it has been associated with hyponatremia (56), and almost 50% of reports of chronic hyponatremia are due to inappropriately elevated secretion of vasopressin (1, 57). Thus, recognizing the causal chain by which aging results in inappropriately increased vasopressin secretion may lead to new targets for preventing osteoporosis.

Figure legends

Figure 1. Expression of NK3R (green) in vasopressin cells (magenta) in coronal sections of the rat SON (A,B) and PVN (C,D). B and D are enlarged views of the highlighted square areas indicated in the right panels of A and C. The white arrows indicate examples of cells in which NK3R and vasopressin-neurophysin (VP-NP) immunoreactivity co-localize. Note the expression of NK3R in fibres and cell membranes highlighted in the cell arrowed in D. 3V, third ventricle; OC, optic chiasm.

Figure 2. Expression of NK3R (green) in oxytocin cells (magenta) in coronal sections of the rat SON (A) and PVN C). B and D are enlarged views of the highlighted square areas indicated in the right panels of A and C. The white arrows indicate examples of cells in which NK3R and oxytocin-neurophysin (OT-NP) immunoreactivity co-localize. Note the expression of NK3R in axons and cell membranes highlighted in the cells arrowed in D. OC, optic chiasm; 3V, third ventricle.

Figure 3. (A) NKB (green) and vasopressin-neurophysin (VP-NP; magenta) immunoreactivity in a coronal section of the rat anterior hypothalamus. Note that NKB fibres project from the rostral arcuate nucleus laterally towards the SON, and dorsally towards the PVN. NKB-expressing fibres (green) are apparent in coronal sections of the SON (B) and PVN (C). These fibres were found in close juxtaposition to vasopressin cells in both the SON (B) and PVN (C). The panels to the right show enlarged views of the marked square area. OC, optic chiasm; ME, median eminence; 3V, third ventricle.

Figure 4. (A) Coronal section of the rat SON showing the injection site of retro-beads (magenta). (B) Coronal section showing an example of localization of NKB (green) and retro-beads (magenta) in the arcuate nucleus following injection of retro-beads in the rat SON. (C) Enlarged view of (B) showing a cell (white arrow) that contains a large number of beads but no NKB and a cell that expresses NKB and contains a few beads (yellow arrow) D shows the cell in C taken at a different focal plane showing these beads clearly within the cell. E shows another example of a an NKB-expressing cell containing beads, and F gives a 3D reconstruction of the cell shown in (E), illustrating how we confirmed the presence of beads within cells. TD, transmitted light channel; OC, optic chiasm.

Figure 5. A coronal section of the arcuate nucleus in a *kiss1*-Cre/eGFP mouse showing kisspeptin cells labeled with YFP (yellow). Background staining with nuclear marker Hoechst (blue). B shows kisspeptin projections (yellow) and vasopressin-neurophysin (VP-NP; magenta) immunoreactivity in coronal sections of the *kiss1*-Cre/eGFP mice in the SON (B) and PVN (C). The panels on the right are enlargements of the white squares indicated in the panels to the left, and show YFP-containing fibres in close juxtaposition to vasopressin cells. 3V, third ventricle; OC, optic chiasm.

Figure 6. Changes in electrical activity in magnocellular vasopressin and oxytocin neurones of the SON in response to i.c.v. injection of senktide (600 pmol in 2μl) *in vivo*. (A) Representative recording showing the increase in electrical activity in a phasically firing vasopressin neurone in response to senktide: the firing rate is plotted in 1-s bins. (B) Mean (SE) hazard functions for vasopressin (white circles) and oxytocin neurones (black diamonds). (C) Mean (SE) change in firing rate per 10-min bins in vasopressin (white circles) and oxytocin neurones (black diamonds); (D) Extract of voltage recording showing individual spikes; the extract is from the portion of the recording indicated by the dotted lines. (E) Mean change in activity quotient in phasic vasopressin neurones; (F) Mean change in intraburst frequency in phasic vasopressin neurones.
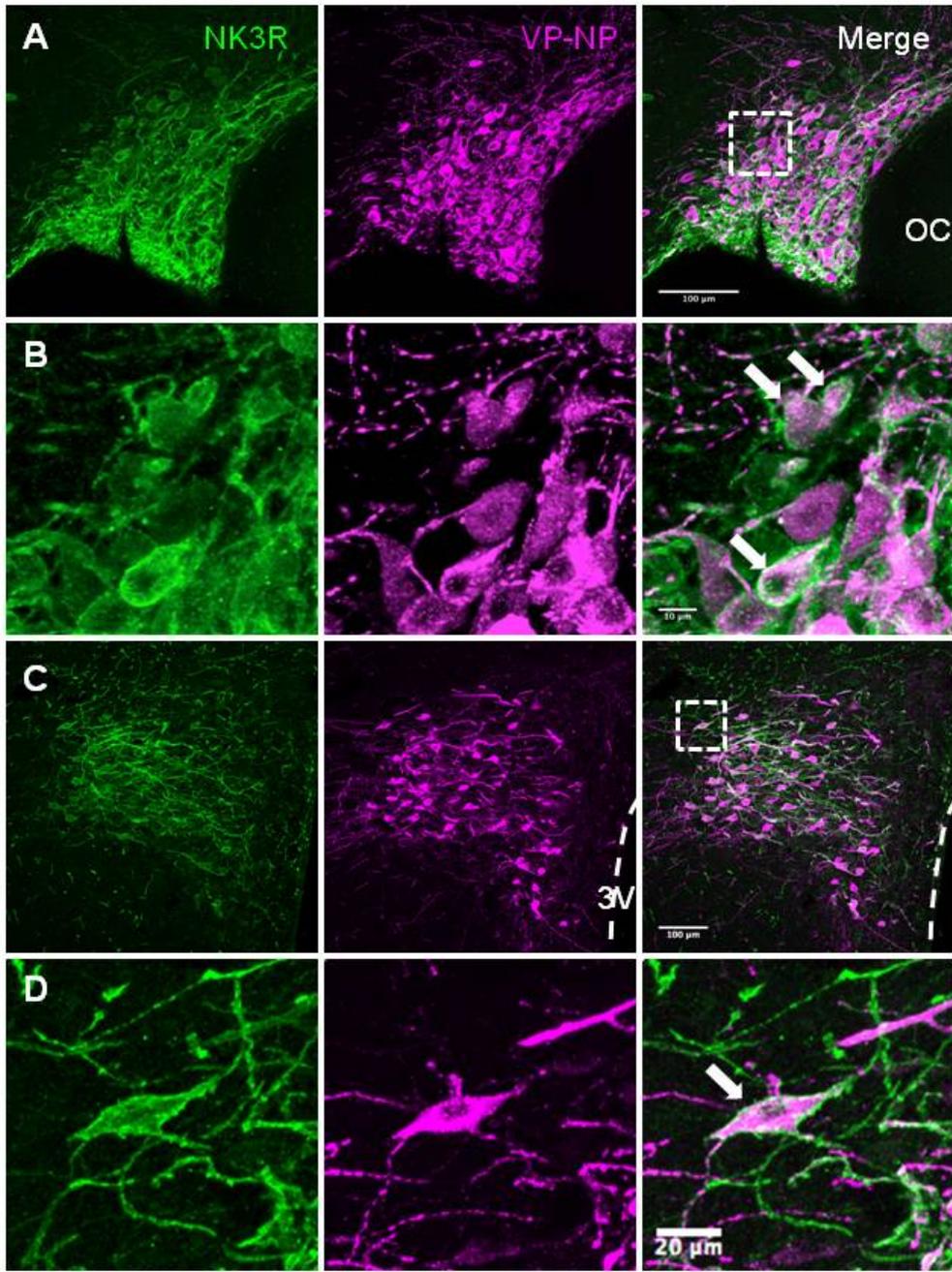
References

1.   Anderson RJ, Chung HM, Kluge R, Schrier RW. Hyponatremia: a prospective analysis of its epidemiology and the pathogenetic role of vasopressin. *Ann Intern Med* 1985; **102:** 164-168.

2.   Fliers E, Swaab DF, Pool CW, Verwer RW. The vasopressin and oxytocin neurons in the human supraoptic and paraventricular nucleus; changes with aging and in senile dementia. *Brain Res* 1985; **342:** 45-53.

3.   Tamma G, Goswami N, Reichmuth J, De Santo NG, Valenti G. Aquaporins, vasopressin, and aging: current perspectives. *Endocrinology* 2015; **156:** 777-788.

4.   Swaab DF. Ageing of the human hypothalamus. *Horm Res* 1995; **43:** 8-11.

5.   Stachenfeld NS. Hormonal changes during menopause and the impact on fluid regulation. *Reprod Sci* 2014; **21:** 555-561.

6.   Almeida TA, Rojo J, Nieto PM, Pinto FM, Hernandez M, Martin JD, et al. Tachykinins and tachykinin receptors: structure and activity relationships. *Curr Med Chem* 2004; **11:** 2045-2081.

7.   Rance NE, Young WS, 3rd. Hypertrophy and increased gene expression of neurons containing neurokinin-B and substance-P messenger ribonucleic acids in the hypothalami of postmenopausal women. *Endocrinology* 1991; **128:** 2239-2247.

8.   Molnar CS, Vida B, Sipos MT, Ciofi P, Borsay BA, Racz K, et al. Morphological evidence for enhanced kisspeptin and neurokinin B signaling in the infundibular nucleus of the aging man. *Endocrinology* 2012; **153:** 5428-5439.

9.   Navarro VM, Castellano JM, McConkey SM, Pineda R, Ruiz-Pino F, Pinilla L, et al. Interactions between kisspeptin and neurokinin B in the control of GnRH secretion in the female rat. *Am J Physiol Endocrinol Metab* 2011; **300:** E202-210.

10.   Sandoval-Guzman T, Stalcup ST, Krajewski SJ, Voytko ML, Rance NE. Effects of ovariectomy on the neuroendocrine axes regulating reproduction and energy balance in young cynomolgus macaques. *J Neuroendocrinol* 2004; **16:** 146-153.

11.   Cholanian M, Krajewski-Hall SJ, McMullen NT, Rance NE. Chronic oestradiol reduces the dendritic spine density of KNDy (kisspeptin/neurokinin B/dynorphin) neurones in the arcuate nucleus of ovariectomised Tac2-enhanced green fluorescent protein transgenic mice. *J Neuroendocrinol* 2015; **27:** 253-263.

12.   Saigo A, Takano Y, Matsumoto T, Tran M, Nakayama Y, Saito R, et al. Central administration of senktide, a tachykinin NK-3 agonist, has an antidiuretic action by stimulating AVP release in water-loaded rats. *Neurosci Lett* 1993; **159:** 187-190.

13.   Eguchi T, Takano Y, Hatae T, Saito R, Nakayama Y, Shigeyoshi Y, et al. Antidiuretic action of tachykinin NK-3 receptor in the rat paraventricular nucleus. *Brain Res* 1996; **743:** 49-55.

14.   Howe HE, Somponpun SJ, Sladek CD. Role of neurokinin 3 receptors in supraoptic vasopressin and oxytocin neurons. *J Neurosci* 2004; **24:** 10103-10110.

15.   Haley GE, Flynn FW. Tachykinin NK3 receptor contribution to systemic release of vasopressin and oxytocin in response to osmotic and hypotensive challenge. *Am J Physiol Regul Integr Comp Physiol* 2007; **293:** R931-937.

16.   Vercelli A, Repici M, Garbossa D, Grimaldi A. Recent techniques for tracing pathways in the central nervous system of developing and adult mammals. *Brain Res Bull* 2000; **51:** 11-28.

17.   Cetin A, Komai S, Eliava M, Seeburg PH, Osten P. Stereotaxic gene delivery in the rodent brain. *Nat Protoc* 2006; **1:** 3166-3173.

18.   Paxinos G, Watson C. *The Rat Brain Stereotaxic Coordinates*, 6th Edn. San Diego, CA: Academic Press, 2006.

19.   Kuhlman SJ, Huang ZJ. High-resolution labeling and functional manipulation of specific neuron types in mouse brain by Cre-activated viral gene expression. *PLoS One* 2008; **3:** e2005.

20.   Zhang F, Gradinaru V, Adamantidis AR, Durand R, Airan RD, de Lecea L, et al. Optogenetic interrogation of neural circuits: technology for probing mammalian brain structures. *Nat Protoc* 2010; **5:** 439-456.

21.   Burke MC, Letts PA, Krajewski SJ, Rance NE. Coexpression of dynorphin and neurokinin B immunoreactivity in the rat hypothalamus: Morphologic evidence of interrelated function within the arcuate nucleus. *J Comp Neurol* 2006; **498:** 712-726.

22.   Navarro VM, Gottsch ML, Chavkin C, Okamura H, Clifton DK, Steiner RA. Regulation of gonadotropin-releasing hormone secretion by kisspeptin/dynorphin/neurokinin B neurons in the arcuate nucleus of the mouse. *J Neurosci* 2009; **29:** 11859-11866.

23.   Goodman RL, Lehman MN, Smith JT, Coolen LM, de Oliveira CV, Jafarzadehshirazi MR, et al. Kisspeptin neurons in the arcuate nucleus of the ewe express both dynorphin A and neurokinin B. *Endocrinology* 2007; **148:** 5752-5760.

24.   Ramaswamy S, Seminara SB, Ali B, Ciofi P, Amin NA, Plant TM. Neurokinin B stimulates GnRH release in the male monkey (Macaca mulatta) and is colocalized with kisspeptin in the arcuate nucleus. *Endocrinology* 2010; **151:** 4494-4503.

25.   Gottsch ML, Popa SM, Lawhorn JK, Qiu J, Tonsfeldt KJ, Bosch MA, et al. Molecular properties of Kiss1 neurons in the arcuate nucleus of the mouse. *Endocrinology* 2011; **152:** 4298-4309.
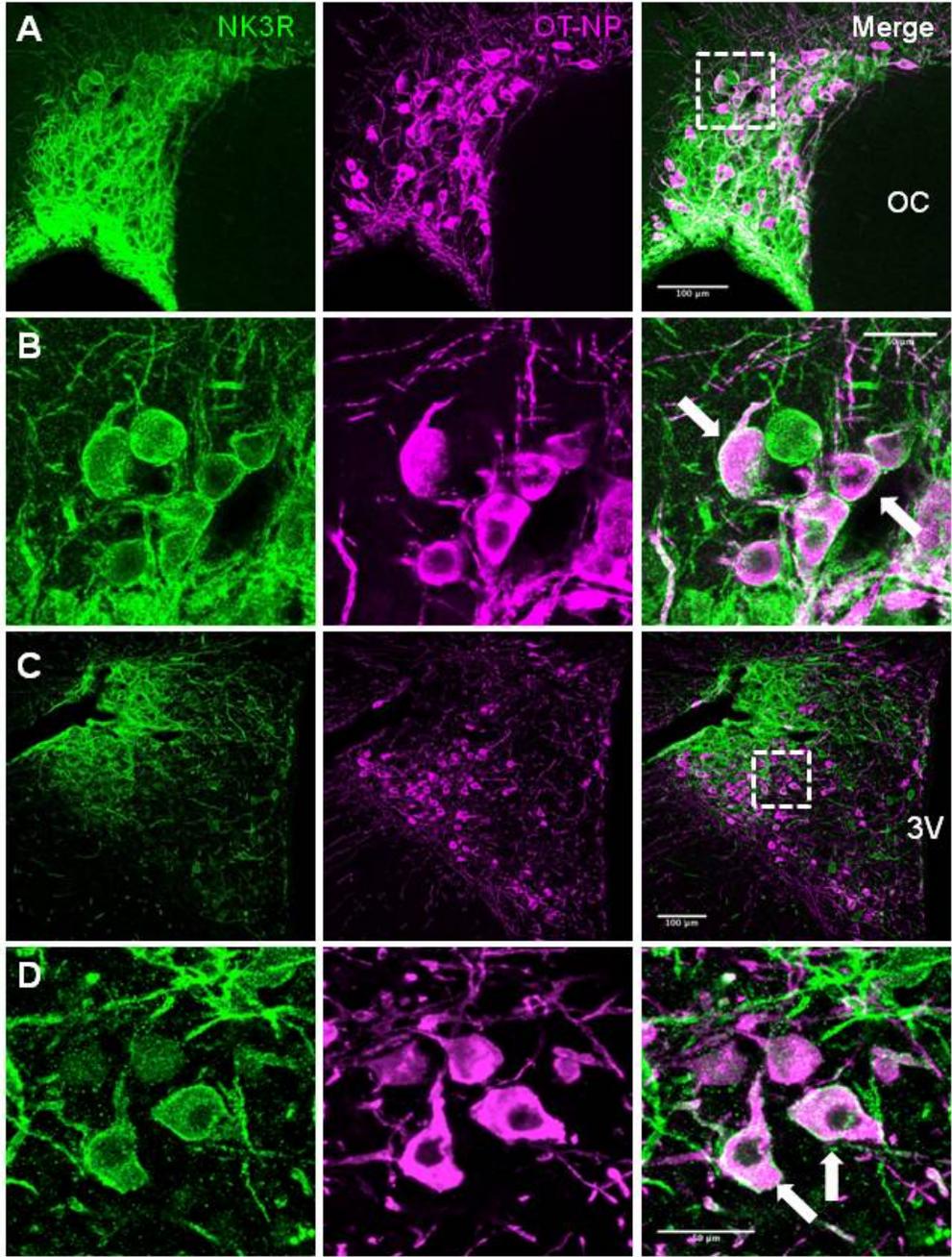
26.   Tsai HC, Zhang F, Adamantidis A, Stuber GD, Bonci A, de Lecea L, et al. Phasic firing in dopaminergic neurons is sufficient for behavioral conditioning. *Science* 2009; **324:** 1080-1084.

27.   Tye KM, Mirzabekov JJ, Warden MR, Ferenczi EA, Tsai HC, Finkelstein J, et al. Dopamine neurons modulate neural encoding and expression of depression-related behaviour. *Nature* 2013; **493:** 537-541.

28.   Paxinos G, Franklin KBJ. *The Mouse Brain in Stereotaxic Coordinates*. Elsevier Academic Press, 2004.

29.   Leng G, Sabatier N. Electrophysiology of Magnocellular Neurons *in vivo*. In Armstrong WE, Tasker JG, eds. Neurophysiology of Neuroendocrine Neurons. John Wiley & Sons, Ltd, UK; 2015: 3-28.

30.   Sabatier N, Brown CH, Ludwig M, Leng G. Phasic spike patterning in rat supraoptic neurones in vivo and in vitro. *J Physiol* 2004; **558:** 161-180.

31.   Ding YQ, Shigemoto R, Takada M, Ohishi H, Nakanishi S, Mizuno N. Localization of the neuromedin K receptor (NK3) in the central nervous system of the rat. *J Comp Neurol* 1996; **364:** 290-310.

32.   Miklos Z, Flynn FW, Lessard A. Stress-induced dendritic internalization and nuclear translocation of the neurokinin-3 (NK3) receptor in vasopressinergic profiles of the rat paraventricular nucleus of the hypothalamus. *Brain Res* 2014; **1590:** 31-44.

33.   Warden MK, Young WS, 3rd. Distribution of cells containing mRNAs encoding substance P and neurokinin B in the rat central nervous system. *J Comp Neurol* 1988; **272:** 90-113.

34.   Lucas LR, Hurley DL, Krause JE, Harlan RE. Localization of the tachykinin neurokinin B precursor peptide in rat brain by immunocytochemistry and in situ hybridization. *Neuroscience* 1992; **51:** 317-345.

35.   Marksteiner J, Sperk G, Krause JE. Distribution of neurons expressing neurokinin B in the rat brain: immunohistochemistry and in situ hybridization. *J Comp Neurol* 1992; **317:** 341-356.

36.   Hatae T, Kawano H, Karpitskiy V, Krause JE, Masuko S. Arginine-vasopressin neurons in the rat hypothalamus produce neurokinin B and co-express the tachykinin NK-3 receptor and angiotensin II type 1 receptor. *Arch Histol Cytol* 2001; **64:** 37-44.

37.   Polidori C, Saija A, Perfumi M, Costa G, de Caro G, Massi M. Vasopressin release induced by intracranial injection of tachykinins is due to activation of central neurokinin-3 receptors. *Neurosci Lett* 1989; **103:** 320-325.

38.   Ding YD, Shi J, Su LY, Xu JQ, Su CJ, Guo XE, et al. Intracerebroventricular injection of senktide-induced Fos expression in vasopressin-containing hypothalamic neurons in the rat. *Brain Res* 2000; **882:** 95-102.

39.   Bealer SL, Flynn FW. Central neurokinin 3 receptors increase systemic oxytocin release: interaction with norepinephrine. *Exp Neurol* 2003; **184:** 1027-1033.

40.   Haley GE, Flynn FW. Agonist and hypertonic saline-induced trafficking of the NK3-receptors on vasopressin neurons within the paraventricular nucleus of the hypothalamus. *Am J Physiol Regul Integr Comp Physiol* 2006; **290:** R1242-1250.

41.   Jensen D, Zhang Z, Flynn FW. Trafficking of tachykinin neurokinin 3 receptor to nuclei of neurons in the paraventricular nucleus of the hypothalamus following osmotic challenge. *Neuroscience* 2008; **155:** 308-316.

42.   Flynn FW, Jensen DD, Thakar A, Xu X, Flynn SW, Zhang Z. Neurokinin 3 receptor forms a complex with acetylated histone H3 and H4 in hypothalamic neurons following hyperosmotic challenge. *Am J Physiol Regul Integr Comp Physiol* 2011; **301:** R822-831.

43.   Douglas AJ, Bicknell RJ, Leng G, Russell JA, Meddle SL. Beta-endorphin cells in the arcuate nucleus: projections to the supraoptic nucleus and changes in expression during pregnancy and parturition. *J Neuroendocrinol* 2002; **14:** 768-777.

44.   Sawchenko PE, Swanson LW, Joseph SA. The distribution and cells of origin of ACTH(1-39)-stained varicosities in the paraventricular and supraoptic nuclei. *Brain Res* 1982; **232:** 365-374.

45.   Leng G, Yamashita H, Dyball RE, Bunting R. Electrophysiological evidence for a projection from the arcuate nucleus to the supraoptic nucleus. *Neurosci Lett* 1988; **89:** 146-151.

46.   Ludwig M, Leng G. GABAergic projection from the arcuate nucleus to the supraoptic nucleus in the rat. *Neurosci Lett* 2000; **281:** 195-197.

47.   Ludwig M, Brown CH, Russell JA, Leng G. Local opioid inhibition and morphine dependence of supraoptic nucleus oxytocin neurones in the rat in vivo. *J Physiol* 1997; **505:** 145-152.

48.   Scott V, Brown CH. Kisspeptin activation of supraoptic nucleus neurons in vivo. *Endocrinology* 2011; **152:** 3862-3870.

49.   Scott V, Brown CH. Beyond the GnRH axis: kisspeptin regulation of the oxytocin system in pregnancy and lactation. *Adv Exp Med Biol* 2013; **784:** 201-218.

50.   True C, Kirigiti M, Ciofi P, Grove KL, Smith MS. Characterisation of arcuate nucleus kisspeptin/neurokinin B neuronal projections and regulation during lactation in the rat. *J Neuroendocrinol* 2011; **23:** 52-64.

51.   Brown CH, Bains JS, Ludwig M, Stern JE. Physiological regulation of magnocellular neurosecretory cell activity: integration of intrinsic, local and afferent mechanisms. *J Neuroendocrinol* 2013; **25:** 678-710.

52.   Sladek CD, Swenson KL, Kapoor R, Sidorowicz HE. The role of steroid hormones in the regulation of vasopressin and oxytocin release and mRNA expression in hypothalamo-neurohypophysial explants from the rat. *Exp Physiol* 2000; **85:** 171S-177S.

53.   Skowsky WR, Swan L, Smith P. Effects of sex steroid hormones on arginine vasopressin in intact and castrated male and female rats. *Endocrinology* 1979; **104:** 105-108.
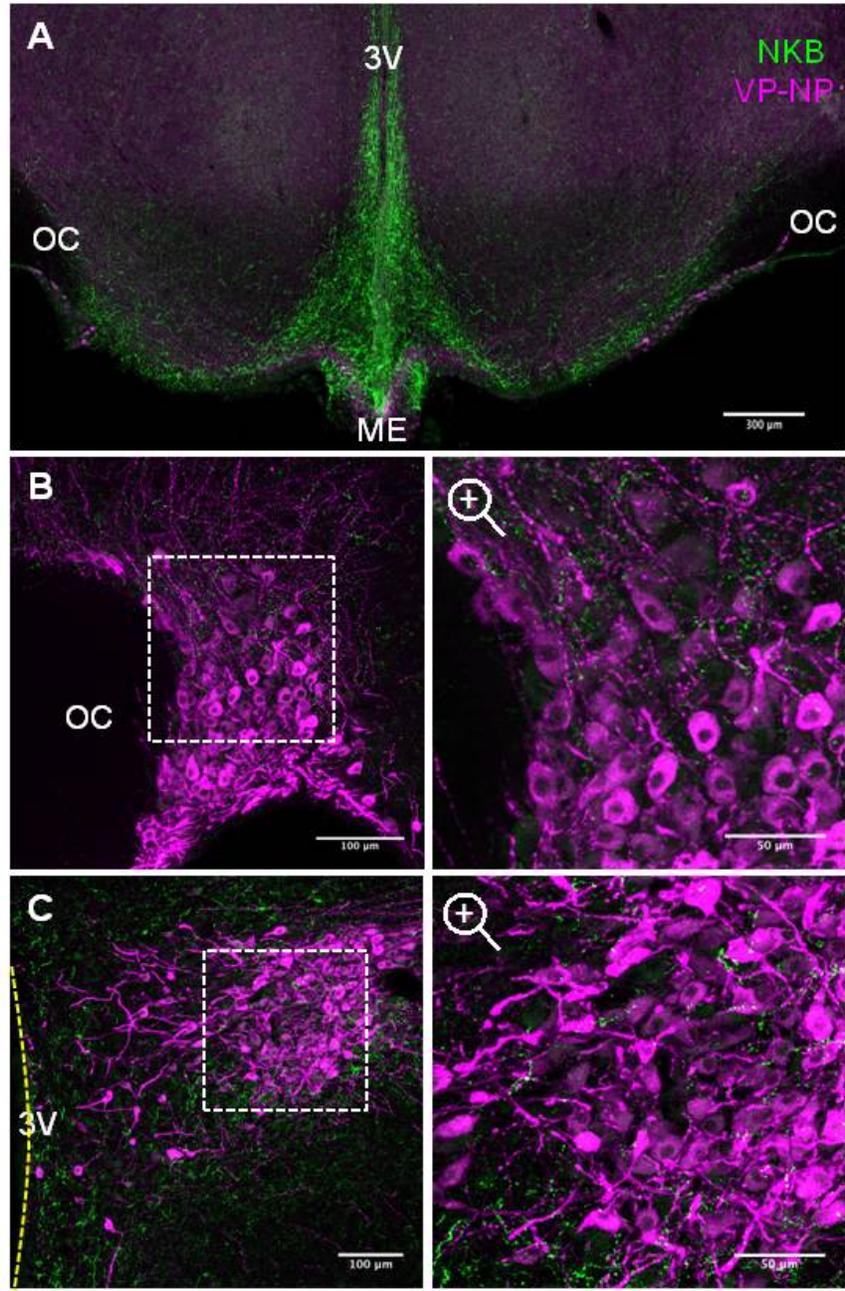
54.   Sauvant J, Delpech JC, Palin K, De Mota N, Dudit J, Aubert A, et al. Mechanisms involved in dual vasopressin/apelin neuron dysfunction during aging. *PLoS One* 2014; **9:** e87421.

55.   Rachner TD, Khosla S, Hofbauer LC. Osteoporosis: now and the future. *Lancet* 2011; **377:** 1276-1287.

56.   Verbalis JG, Barsony J, Sugimura Y, Tian Y, Adams DJ, Carter EA, et al. Hyponatremia-induced osteoporosis. *J Bone Miner Res* 2010; **25:** 554-563.

57.   Gross PA, Pehrisch H, Rascher W, Schomig A, Hackenthal E, Ritz E. Pathogenesis of clinical hyponatremia: observations of vasopressin and fluid intake in 100 hyponatremic medical patients. *Eur J Clin Invest* 1987; **17:** 123-129.
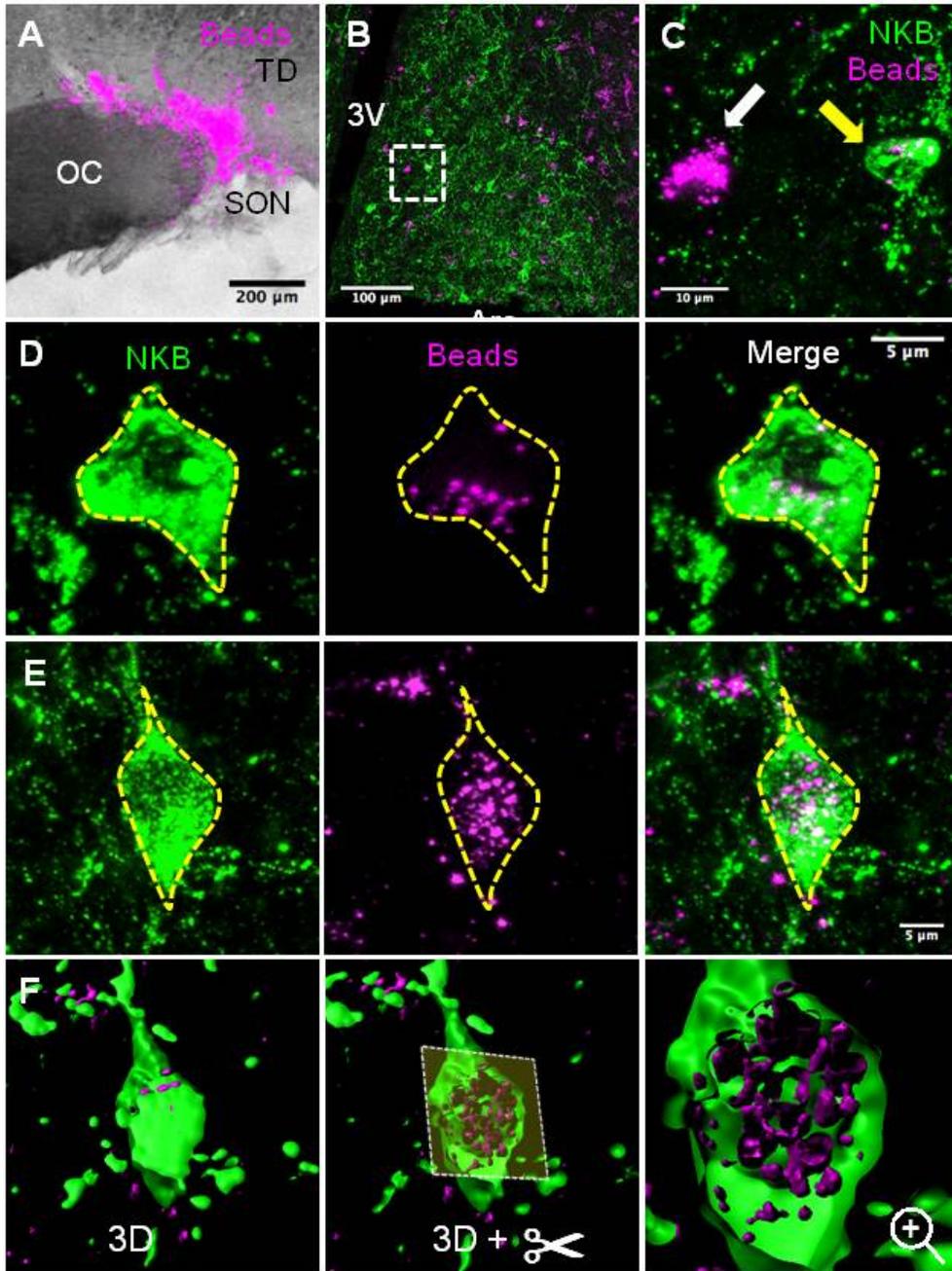
NK3R   VP-NP   Merge
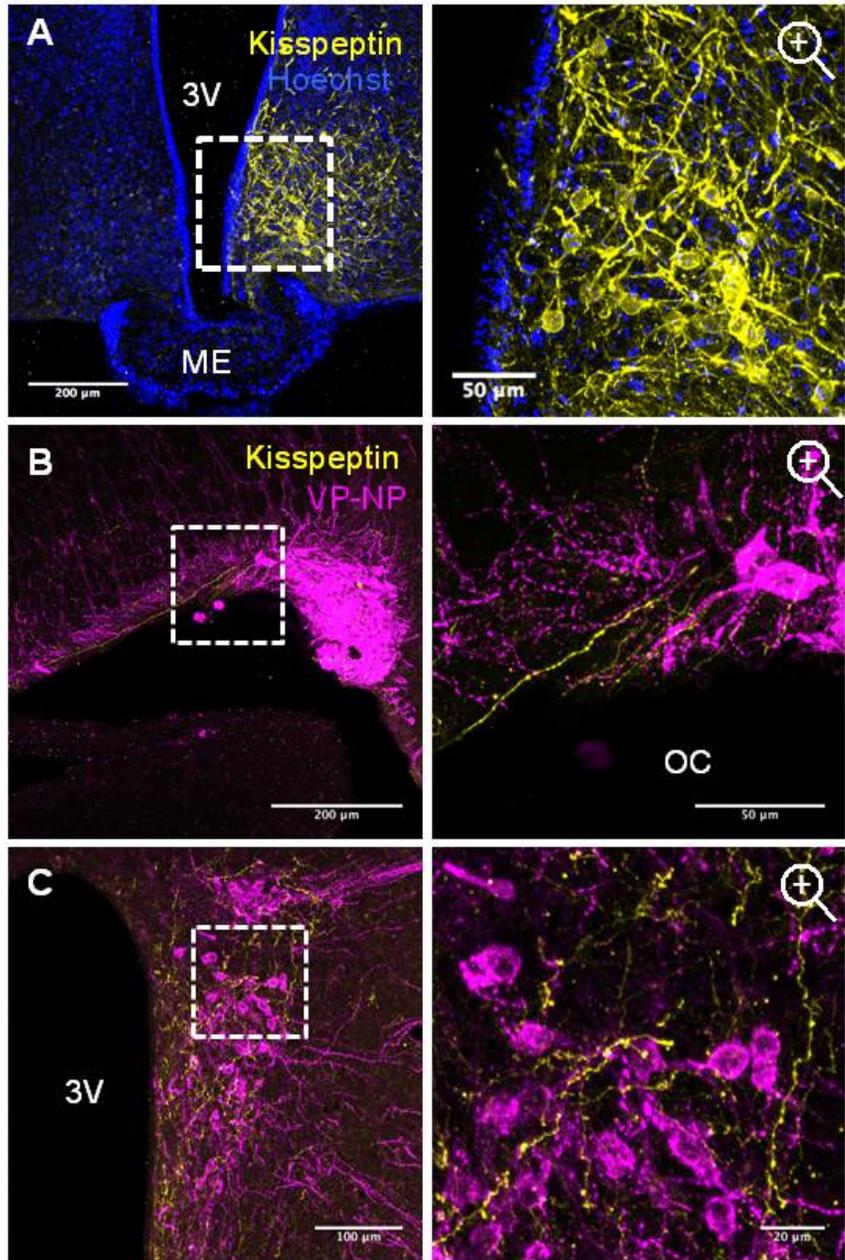
A   OC

B

C   3V

D   20 μm

Pineda et al., Fig 1

NK3R   OT-NP   Merge

A   OC

B

C   3V

D

Pineda et al., Fig 2

A
3V
OC
OC
NKB
VP-NP
ME
300 μm

B
OC
100 μm
50 μm

C
3V
100 μm
50 μm

Pineda et al., Fig 3

A — Beads, TD, OC, SON — 200 μm

B — 3V, 100 μm

C — NKB, Beads — 10 μm

D — NKB | Beads | Merge — 5 μm

E — 5 μm

F — 3D | 3D + ✂ | ⊕

Pineda et al., Fig 4

Pineda et al., Fig 5

A

Firing rate (spikes/s)

Senktide

5 min

B

Mean hazard

○ Vasopressin cells
◆ Oxytocin cells

Time (s)

C

Mean change in firing rate (spikes/s)

Time since Senktide (min)

D

mV

2 s

Activity quotient (%)

Time since Senktide (min)

Intraburst frequency (%)

Time since Senktide (min)

Pineda et al., Fig 6